Available online at www.sciencedirect.com
ScienceDirect
Trans. Nonferrous Met. Soc. China 35(2025) 3869−3885
Transactions of Nonferrous Metals Society of China
www.tnmsc.cn

Smelting separation behaviors of various reduced vanadium titanomagnetite pellets

Zheng-qi GUO[1], Xing CHEN[1], Yue SHI[2], De-qing ZHU[1], Jian PAN[1], Cong-cong YANG[1], Si-wei LI[1], Ji-wei XU[1], Xin WANG[1]

1. School of Minerals Processing and Bioengineering, Central South University, Changsha 410083, China;
2. School of Materials Science and Engineering, Henan University of Science and Technology, Luoyang 471000, China

Received 24 October 2024; accepted 15 June 2025

Abstract: The melting and separation behavior of vanadium−titanium magnetite pellets directed at an efficient extraction of vanadium and titanium was systematically investigated. Applying FactSage simulations and experiments, the smelting separation of three pre-reduced pellets from different regions was analyzed. The simulations demonstrate that $FeTi_2O_5$ is converted to TiC at low temperatures, necessitating suppression of this step. Experiments under optimized conditions (1590−1690 °C, 20−25 min, 2% coke, basicity 0.4−0.6, and 3.0%−6.0% MgO) yield iron grade of 92.35%−95.06%, titanium grade of 34.37%−39.89%, and vanadium grade of 0.56%−1.52%, with recoveries of 99.52%−99.60%, 94.08%−98.96%, and 92.63%−94.38% for iron, titanium and vanadium, respectively. The titanium in the slag, primarily in the form of anosovite, is suitable for sulfuric acid-based titanium white production. An increase in basicity, MgO content, and pellet metallization serves to improve vanadium recovery in melted iron but lowers the titanium grade in the slag. The overall process effectively utilizes vanadium and titanium resources under optimized conditions.
Key words: vanadium titanomagnetite; pellet pre-reduction; smelting separation; titanium slag utilization

1 Introduction

Vanadium titanomagnetite (VTM) is a polymetallic co-associated iron ore resource with a significant utilization value. The main ore enrichment elements are iron, vanadium, and titanium, with chromium, cobalt, nickel, and copper. Global reserves exceed 40 billion tons, and its strategic application has assumed increasing importance [1,2]. Currently, VTM treatment is largely reliant on blast furnace-converter processing. In VTM smelting, the raw ore undergoes beneficiation to produce a vanadium and titanium concentrate, which, following a briquetting-roasting process, is smelted in a blast furnace. The majority of the vanadium oxides are reduced to melted iron, and the titanium oxides are incorporated into the slag [3−5]. Vanadium-bearing molten iron is conveyed through the converter to produce vanadium slag and semi-steel. The vanadium slag is then subjected to a wet vanadium extraction to obtain the requisite vanadium products. The semi-steel is subsequently subjected to further refining processes in order to obtain a qualified steel product [6−8]. The blast furnace process exhibits a number of disadvantages, including lengthy process flow, appreciable environmental pollution and the requirement for substantial infrastructure investment. Furthermore, recycling of blast furnace slag is hindered by the low TiO_2 content (<25%), complex mineral composition and the prevalence of glass phases. Consequently, blast furnace slag typically constitutes waste, contributing

Corresponding author: Yue SHI, Tel: +86-15211077651, E-mail: shiyue@haust.edu.cn
https://doi.org/10.1016/S1003-6326(25)66918-4

to environmental pollution and an inefficient use of resources [7,9,10]. In response to these drawbacks, a significant effort has been made to develop non-blast furnace smelting processes, tailored to specific circumstances, with the objective of recovering vanadium and titanium from VTM. This has resulted in a detailed examination of low-carbon "green" metallurgy and the recovery of valuable metals, which has included hydrogen-based reduction, selective reduction and separation techniques. The pre-reduction smelting of VTM still faces a number of challenges. Although hydrogen-based reduction works well in the laboratory, industrial application is constrained by such factors as the cost of hydrogen, safe storage, and the optimized design of large-scale equipment and units. Moreover, the fine grain size and complex intergrowth associated with VTM present technical difficulties in smelting and separation processes. Currently, the most extensively studied and applied non-blast furnace systems include reduction-grinding-separation, pre-reduction-electric furnace, and sodium-enhanced vanadium extraction processes [11−14]. The pre-reduction- electric furnace process is characterized by relatively simple smelting operation, minimal environmental impact, short processing time, and high efficiency, offering economic benefits and facilitating sustainable low-carbon development. This now represents the dominant approach to comprehensive VTM utilization, with extensive deployment in South Africa and New Zealand [15−17].

The VTM pre-reduction pellet smelting process is a pivotal component of the direct reduction electric furnace smelting separation process. It facilitates the separation of valuable elements and titanium-containing slag, while enabling the reduction of iron and vanadium and the production of clean vanadium-containing molten iron and titanium slag during slag-iron separation [18,19]. Progress in VTM pre-reduction pellet smelting separation has delivered effective slag-iron separation. However, a precise control of vanadium and titanium distribution requires further process improvements, with enhanced vanadium recovery from melted iron being a priority issue. Most VTM smelting separation processes require high slag basicity, which invariably lowers the TiO_2 grade in the slag [20−22]. In addition, the titanium slag often contains high levels of impurities, notably calcium and silicon. When these slags are used in titanium dioxide production using the sulfuric acid process, the impurities interfere with slag decomposition and settling, leading to the accumulation of substantial waste slag [23].

Current optimization of titanium slag for VTM has focused on adjusting slag composition to promote the formation of a low-melting-point phase, enhancing the titanium grade. JIAO et al [24] showed that an increase in TiO_2 content results in a reduction in slag viscosity, where TiO_2 exhibits high bond lengths and low bond energies. ZHOU et al [25] demonstrated that titanium viscosity significantly decreased with an increasing CaO/SiO_2 ratio from 0.1 to 0.8. It is therefore necessary to address the coordination of the pre-reduction process with the reduction smelting separation, as well as the titanium slag upgrading process in order to fully establish the factors affecting the iron, vanadium and titanium components.

In this study, the smelting separation behaviors of three pre-reduced VTM pellets from different regions were systematically investigated. The effects of the smelting separation process and different slag types on the ultimate iron, vanadium and titanium components were studied, and the findings can inform the production of high-quality vanadium-bearing molten iron and titanium slag by smelting separation in VTM electric furnaces.

2 Experimental

2.1 Raw materials

Three VTM samples were used to prepare the pre-reduced pellets, denoted as pellet 1, pellet 2, and pellet 3. The strength of all pellets was 2500 N and the chemical compositions are listed in Table 1. Both pellet 1 and pellet 3 can be categorized as high-titanium VTM pellets, with TiO_2 contents of 14.29 % and 11.40 %, respectively. The content of valuable metal (TiO_2 and V_2O_5) in pellet 1 is slightly higher than that of pellet 3. The total iron (TFe) content of pellet 2 has the highest grade (79.04%), and the V_2O_5 and TiO_2 contents are 0.94% and 7.22%, respectively. The TiO_2 content is significantly lower than the other two ores, which may lead to a lower TiO_2 grade in the smelting slag. In addition, the impurity contents (SiO_2, CaO,

Table 1 Chemical composition of three pre-reduced VTM pellets (wt.%)

Pellet	TFe	MFe	TiO_2	V_2O_5	CaO	SiO_2	MgO	Al_2O_3	K_2O	Na_2O	P	S
1	66.32	59.31	14.29	1.95	0.23	6.19	1.68	5.49	0.15	0.20	0.009	0.011
2	79.04	67.07	7.22	0.94	0.27	2.49	1.19	3.88	0.017	0.16	0.021	0.026
3	67.75	56.17	11.40	0.85	0.50	5.99	4.57	4.60	0.033	0.36	0.0085	0.025

MgO, and Al_2O_3) in pellets 1, 2, and 3 are 13.59 %, 7.83 %, and 15.66 %, respectively.

The X-ray diffraction (XRD) patterns of the three reduced pellets are shown in Fig. 1. The main phases in each case are metallic iron and ilmenite, with some differences with respect to magnesium anosovite in pellet 1 and magnesium titanate in pellets 2 and 3. As can be seen from the optical images given in Fig. 2, the metallic iron particles present in pellet 1 exhibit a fine dispersion with evidence of small pores. The microstructure of pellet 2 is characterized by flakes of ilmenite, with the metallic iron particles exhibiting an acicular and flaky morphology. In addition, there is evidence of iron particle aggregation. The metallic iron particles in pellet 3 are finer, and do not form flakes, exhibiting more holes and cracks, and irregularly shaped silicate minerals. The SEM−EDS analysis results are presented in Fig. 2, where point 1 and point 2 of pellet 1 correspond to the silicate-bonded phase and an ilmenite phase, respectively. The ilmenite phase exhibits a worm-like distribution with large metallic iron particles at the edges. The fine-grained metallic iron in pellet 2 is concentrated at the edges of the minerals. In addition, there is evidence of metallic iron present as sheets. Analysis of point 2 indicates that the worm-like metallic iron contains trace quantities of titanium, and the silicate exhibits a minor vanadium component. In the case of pellet 3, the silicate is bonded to the metallic iron particles, but there is no evidence of aggregation to form sheets. The vanadium content at point 2 is slightly high.

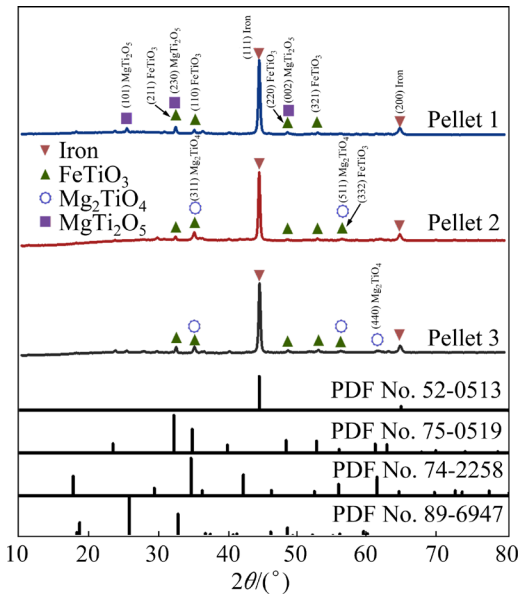

Fig. 1 XRD patterns of three pre-reduced VTM pellets

The coke used as the reducing agent had a fixed carbon content of 52.12%, a volatile matter content of 30.41%, an ash content of 4.49%, and a sulfur content of 0.34%.

2.2 Experimental procedures

The VTM pre-reduced smelting separation experiments were conducted using an electro-magnetic induction furnace (SP-50KTC), as illustrated in Fig. 3. Firstly, the pellets (1, 2 and 3), which exhibited 89%, 85% and 83% degrees of metallization, respectively, were pulverized to a particle size of less than 1 mm. In each experiment, 200 g metalized pellet powder was used with the addition of the requisite quantities of MgO and coke powder for the designed slag type. The mixture was blended and transferred to a 50 mL graphite crucible, placed in an induction furnace (380 V and 12 kW), and the timing started when the temperature reached the predetermined point. At the end of the smelting separation experiment, the crucible was removed and placed in a nitrogen atmosphere to prevent oxidation. When the crucible reached ambient temperature, the sample was crushed, and the upper slag layer and lower metal mass were removed and weighed. The metal block was cut into pieces with a cutter, ground finely using a vibratory grinding machine, and assayed for iron, vanadium and titanium content.

Thermodynamic calculations were conducted using the FactSage 8.1 thermodynamic software package, applying the chemical composition of the pellets as the basis for the calculations [26]. The XRD analysis was performed using a Rigaku Ultima

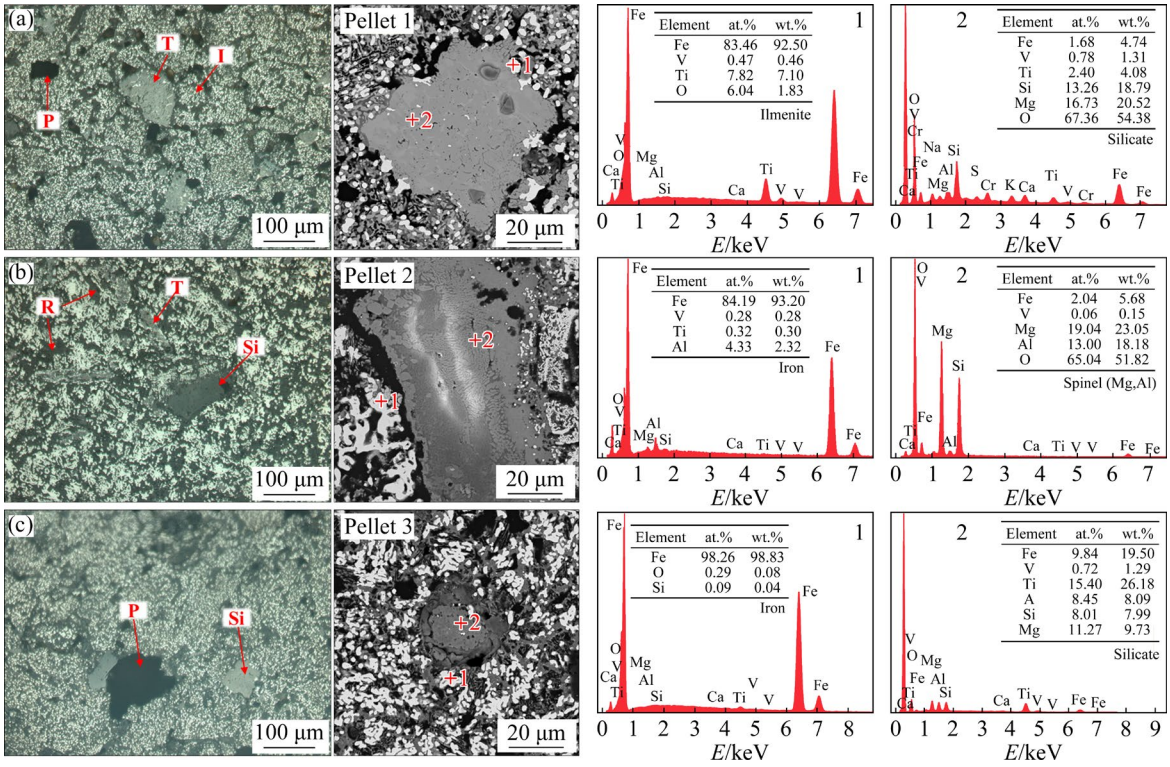

Fig. 2 Optical microstructures and SEM−EDS analysis of three pre-reduced VTM pellets: (a) Pellet 1; (b) Pellet 2; (c) Pellet 3 (T: Ilmenite; Si: Silicate; I: Metallic iron; P: Pore; R: Resin)

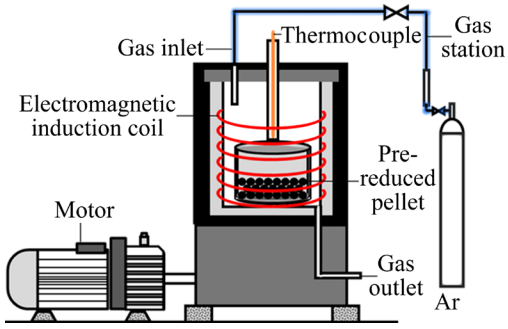

Fig. 3 Schematic representation of electromagnetic induction furnace

IV X-ray diffractometer (Rigaku Corporation, Japan), applying a scanning angle range of 10°−80° (2θ). Peak fitting and phase identification were conducted using MDI Jade 9.0 software to determine the mineral composition of the samples.

3 Thermodynamic analysis

3.1 VTM pellets

3.1.1 Reduction thermodynamics of vanadium-bearing oxides

The vanadium in VTM is gradually reduced when the pellets are smelted in the electric furnace. As vanadium and iron are miscible at elevated temperatures, the vanadium that is reduced at the slag-iron interface does not enter the melted iron as a solid phase, and is dissolved in the melted iron. The vanadium in the spinel phase is also reduced as part of the smelting separation process, forming a vanadium−iron compound with the iron phase [27]. As previously reported in Ref. [28], the reaction of high-valent vanadium oxides with carbon reduction produces low-valent vanadium. The reduction of vanadium oxides follows the order of VC > V_2C > VO > V. Furthermore, excess reductant may be generated in the form of VC and V_2C, which are subsequently dissolved in melted iron.

3.1.2 Reduction thermodynamics of titanium-bearing oxides

The results of thermodynamic calculations have indicated that the reduction of Fe−Ti oxides to metallic iron occurs at relatively low temperatures (about 1000 °C) under standard conditions [29]. The temperature required for the reduction of titanium oxide to TiC is considerably lower than that required for the reduction to TiO_2 and metallic Ti. The crystal structures of different titanium oxides vary, but TiO and TiC are classified as

face-centered cubic crystal systems. As crystal transformation is not required, this lowers the energy requirements of the reaction. In carbothermal reduction, oxygen atoms are readily replaced by carbon atoms, resulting in the formation of TiC [30]. Under standard operating smelting separation temperatures, titanium oxides are reduced in the following order: $FeTi_2O_5 \rightarrow TiO_2 \rightarrow Ti_3O_5 \rightarrow Ti_2O_3 \rightarrow Ti$.

The onset temperatures for the reduction of $CaTiO_3$, Ti_3O_5, $MgTi_2O_5$, TiO_2, and $FeTi_2O_5$ to TiC are 1590.0, 1378.1, 1356.6, 1326.5 and 1219.8 °C, respectively, which are in accordance with the results of previous reports [31]. Differences in the thermodynamic characteristics of vanadium and titanium oxides can be addressed by altering the amount of carbon, incorporating MgO to adjust the slag type. This enables control over the vanadium in the melted iron and titanium in the slag phase during smelting separation.

3.2 Titanium slag

3.2.1 Effect of basicity on liquid phase content and slag viscosity

As shown in Fig. 4, the liquid phase content of pellets 1, 2, and 3 exhibits a gradual increase with increasing temperature. The temperatures at which the slag phase is fully melted are 1540, 1510 and 1450 °C, respectively, under the conditions of natural basicity. The melting temperatures of the three pellets are lowered with an increase in basicity. However, an increase in basicity from 0.4 to 0.8 for pellet 2 results in an increase in the melting temperature from 1390 to 1420 °C. Although increased basicity enables a reduction in melting temperature, a high level of basicity results in a low grade of TiO2 in the slag, which is detrimental to subsequent recycling. Accordingly, the optimal basicities for pellets 1, 2 and 3 are 0.4, 0.4 and 0.6, respectively. Operation at 1600, 1540 and 1540 °C, respectively, is necessary to reduce the viscosities of pellets 1, 2 and 3 to 0.1 Pa·s under conditions of natural basicity. However, the liquid phase viscosity gradually decreases with increasing basicity. In the case of pellet 1 and pellet 2, the temperature required to reach a viscosity of 0.1 Pa·s decreases by an average of approximately 30 °C for each incremental 0.2 increase in basicity. The temperature is 1540 °C when the viscosity of pellet 3 is reduced to below 0.1 Pa·s, and decreases to 1450 °C when the basicity is increased to 0.8. An appropriate increase in basicity facilitates a low viscosity at a given temperature.

3.2.2 Effect of MgO on liquid phase content and slag viscosity

As shown in Fig. 5, the temperatures at which

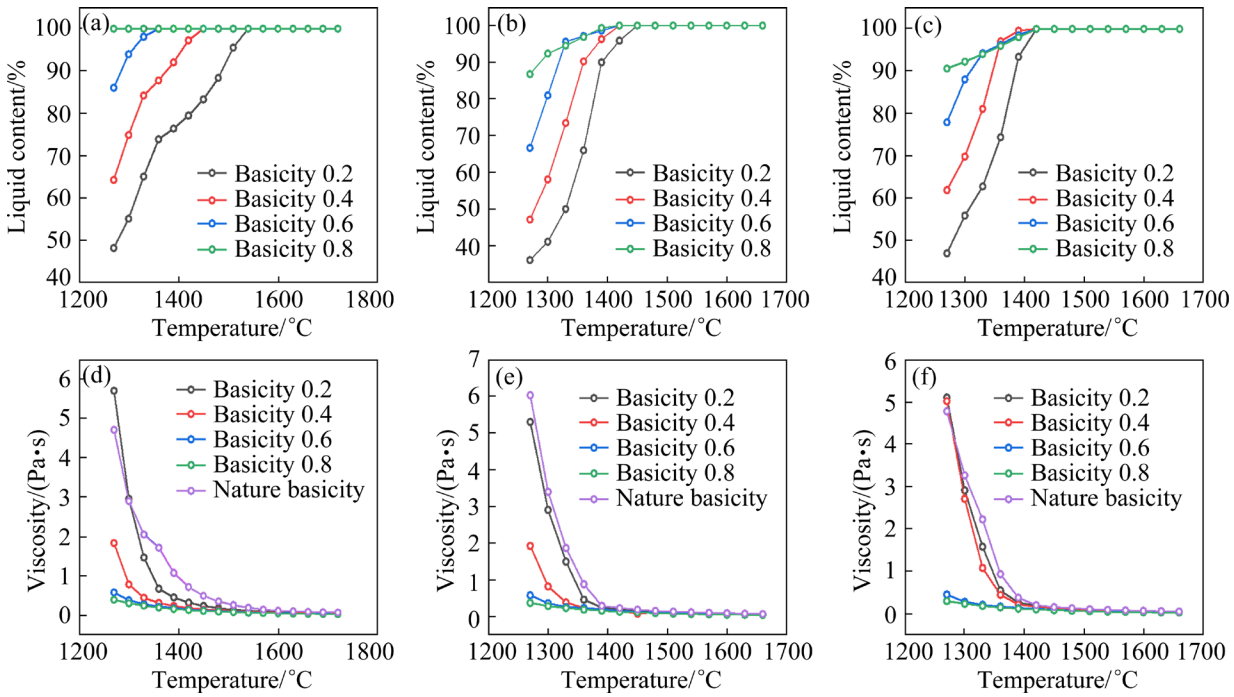

Fig. 4 Effect of basicity on liquid content (a−c) and viscosity (d−f) of simulated slag system: (a, d) Pellet 1; (b, e) Pellet 2; (c, f) Pellet 3

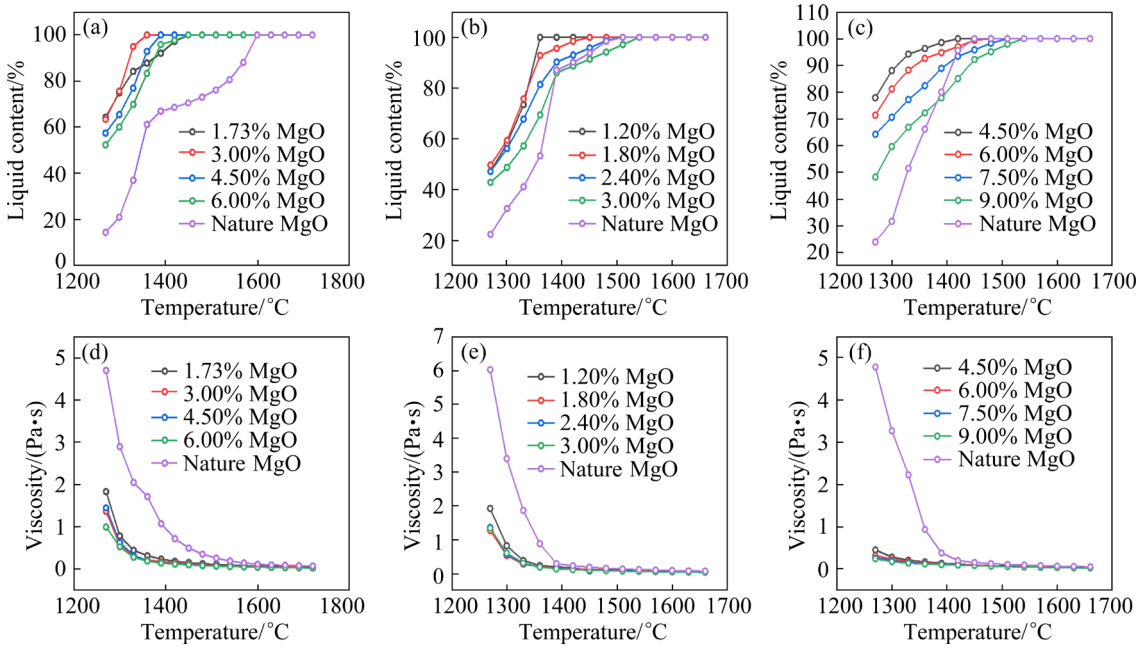

Fig. 5 Effect of MgO content on liquid content (a−c) and viscosity (d−f) of simulated slag system: (a, d) Pellet 1; (b, e) Pellet 2; (c, f) Pellet 3

the slag phase is completely melted under natural basicity for pellets 1, 2 and 3 are 1600, 1510 and 1450 °C, respectively. The melting temperature can be reduced by adding MgO, resulting in significantly low temperatures (1360, 1390 and 1420 °C) for pellets 1, 2 and 3, respectively. The simulation demonstrates that the melting temperature can be reduced by adding MgO, but excess MgO may cause the VTM to become refractory, increasing the amount of slag and diluting the TiO2 content. The viscosity of all three pellets exhibits a decline with increasing MgO content, which is particularly pronounced at low temperatures (1250−1400 °C). The optimal MgO contents for pellets 1, 2, and 3 are 6.0%, 3.0%, and 6.0%, respectively.

The FactSage simulation was conducted to elucidate the compounds associated with the titanium slag, the characteristics during solidification, and the consequent phase equilibrium. The low-melting point region in Fig. 6 is primarily comprised of the $Mg_4Al_{10}Si_2O_{23}$ phase zone, $CaAl_2Si_2O_8$ phase zone, and $CaTiO_3$, Mg_2SiO_4, $MgTi_2O_5$ and TiO_2. During smelting separation, the basicity should be adjusted to 0.4−0.6, while maintaining a MgO content of 17.5%−19% in the slag. This facilitates the generation of $MgTi_2O_5$, $CaTiO_3$, and other titanium-containing oxides with high titanium content.

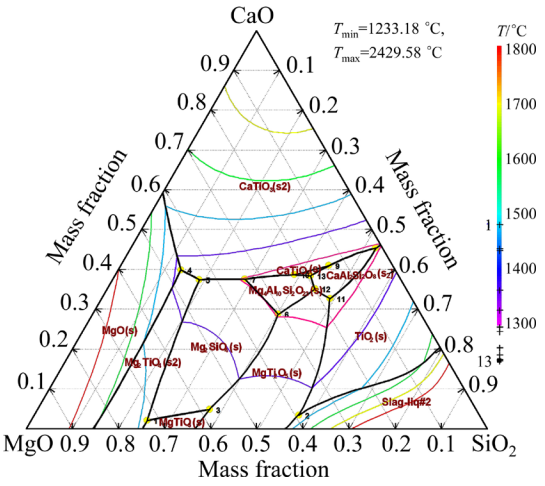

Fig. 6 Phase diagram of CaO−SiO_2−MgO−Al_2O_3−TiO_2 ($m(Al_2O_3)/m(Z)$=0.13, $m(TiO_2)/m(Z)$=0.4, Z=CaO−SiO_2−MgO−Al_2O_3−TiO_2, 1×10^5 Pa)

4 Results and discussion

4.1 Smelting separation process

4.1.1 Effect of reduction temperature

The smelting separation experiments were conducted using powders of pellets 1, 2, and 3 with 89%, 85%, and 83% metallization, respectively, at a melting time of 20 min, with 2% coke powder added and basicity of 0.4. The effect of melting temperature on the smelting separation index is shown in Fig. 7.

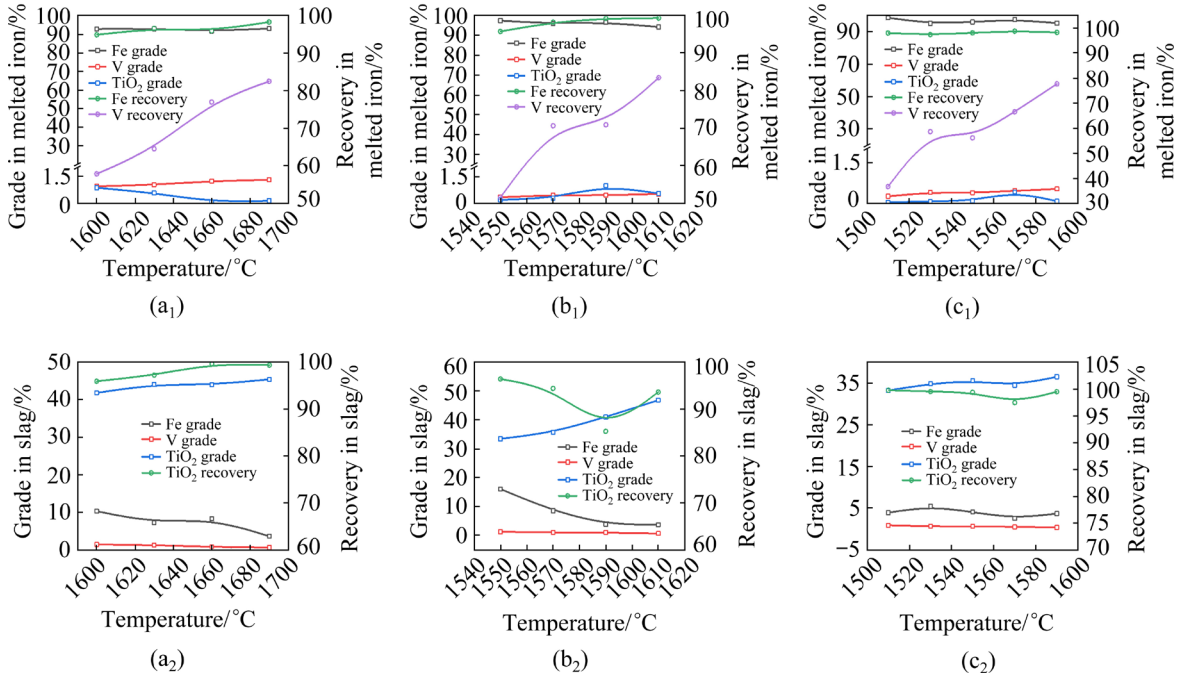

Fig. 7 Effect of temperature on reduction of VTM pellets in melted iron (a_1, b_1, c_1) and in slag (a_2, b_2, c_2): (a_1, a_2) Pellet 1; (b_1, b_2) Pellet 2; (c_1, c_2) Pellet 3

In the case of pellet 1, the iron grade in the slag exhibited a decline from 10.27% to 3.60% with increasing temperature from 1600 to 1690 °C. The vanadium grade in the slag showed a marked decline with increasing temperature, reaching a minimum of 0.62% at 1690 °C. A higher temperature resulted in a decrease in the TiO_2 grade in the melted iron, with the lowest value (0.085%) at 1660 °C. The highest TiO_2 recovery in the slag was 99.59%, with a TiO_2 grade over 41%.

Pellet 2 exhibited an increase in vanadium recovery from 51.62% to 83.48% with an increase in temperature from 1550 to 1610 °C, accompanied by a 0.18% increase in vanadium grade. The vanadium grade in the slag exhibited a marked decline, from 1.22% to 0.60%. The recovery of TiO_2 exhibited the lowest value (81.24%) in the slag at 1590 °C. The TiO_2 grade reached 46.84% at 1610 °C, the iron grade declined with temperature, but the iron recovery rate showed an increase from 95.78% to 99.34%.

In the case of pellet 3, an increase in temperature from 1510 to 1590 °C resulted in an increase in the vanadium grade from 0.26% to 0.53% in melted iron, and an increase in recovery from 36.75% to 77.76%; the vanadium grade decreased from 0.88% to 0.35% in the slag. The iron recovery was maintained at approximately 98% in melted iron. Moreover, the grade of TiO_2 in melted iron first increased and subsequently decreased with increasing temperature, reaching a peak of 0.42% at 1570 °C. In contrast, the grade of TiO_2 in the slag increased with increasing temperature, from 33.24% at 1510 °C to 36.52% at 1590 °C.

The results demonstrate that an increase in temperature facilitates a smooth transition of iron beads and vanadium in the slag to the melted iron phase, whereas TiO_2 remains in the slag. The optimal melting separation temperatures for pellets 1, 2, and 3 are 1690, 1610 and 1590 °C, respectively.

4.1.2 Effect of reduction time

The effect of reduction time on the smelting separation index for pellets 1, 2, and 3 was investigated under optimal conditions, and the results are shown in Fig. 8.

Smelting separation time had a significant effect on vanadium recovery in the case of pellet 1. Extending the reaction time from 10 to 25 min resulted in an increase in the grade of vanadium from 1.08% to 1.41%. The recovery of vanadium reached a maximum (88.61%) at 25 min, and the grade of vanadium in the slag decreased by a factor of 2. The grade of TiO_2 in melted iron exhibited

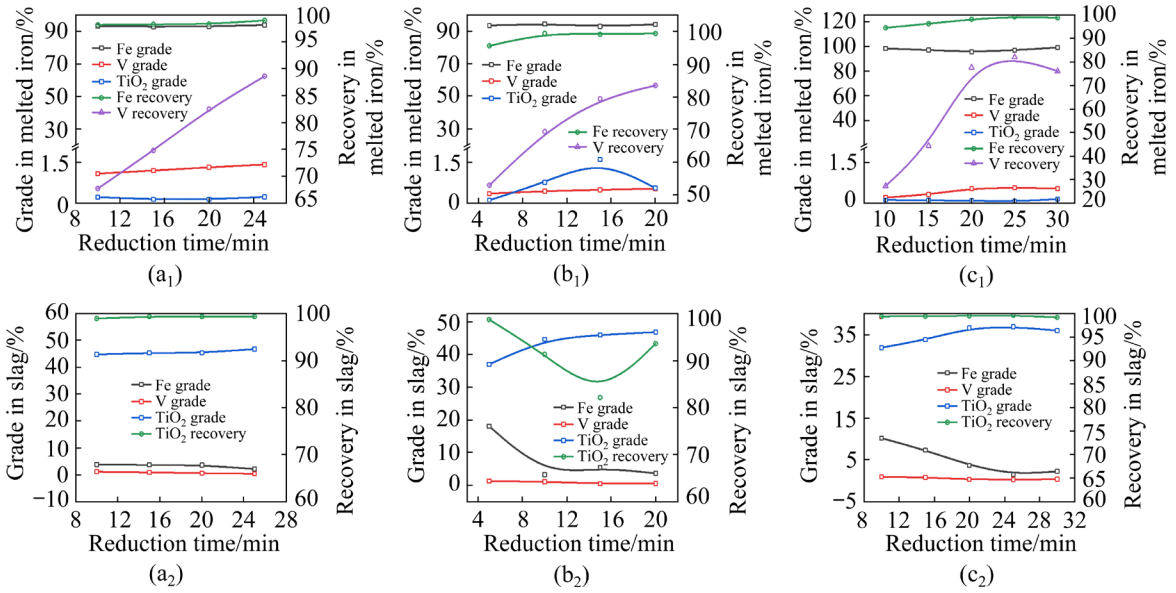

Fig. 8 Effect of reduction time on reduction of VTM pellets in melted iron (a_1, b_1, c_1) and in slag (a_2, b_2, c_2): (a_1, a_2) Pellet 1; (b_1, b_2) Pellet 2; (c_1, c_2) Pellet 3

an initial slight decrease, followed by an increase. The recovery of TiO_2 in the slag remained at 99.34% when the reaction time exceeded 15 min. However, a prolonged reaction significantly affected the TiO_2 grade in the slag, with a 2% increase after a reaction for 25 min.

In the case of pellet 2, the TiO_2 grade in melted iron reached 1.59% after a reaction time of 15 min, representing an increase by a factor of 15 relative to the initial level. The reduction of titanium oxides in VTM-metallized pellets is a challenging process, as established in the calculations and thermodynamic analysis. As the pellets have an iron grade of 79.04%, they contain a significant liquid iron content that has the capacity to dissolve more solid carbon, enhancing the reduction of titanium oxides [32,33]. Consequently, an increased proportion of titanium was reduced to melted iron at a shorter melting time. Extending time to 20 min resulted in a decrease in the TiO_2 grade in melted iron to 0.55%, where the corresponding TiO_2 recovery in the slag reached 93.62%. This was accompanied by a maximum grade of TiO_2 in the slag (46.84%).

In the case of pellet 3, an extension of the reaction time from 10 to 25 min resulted in an increase in the vanadium grade in melted iron, accompanied by a significant increase in vanadium recovery (from 27.27% to 82.17%). The iron and vanadium grades in the slag exhibited an increase, and the TiO_2 grade decreased when the time was prolonged to 30 min. This response is primarily attributed to the complete reduction of vanadium and iron oxides at extended time. However, prolonged smelting can result in titanium oxide over-reduction, generating TiC and other high-melting-point micro-fine solid particles. This leads to an increase in slag viscosity and poor fluidity, which impedes the migration of metal elements in the slag.

The slag−iron separation results have established optimal time of 25, 20, and 25 min for pellets 1, 2, and 3, respectively.

4.1.3 Effect of coke dosage

The effects of coke dosage were investigated for each pellet in the optimal conditions, and the results are presented in Fig. 9.

In the case of pellet 1, the recovery of vanadium in melted iron fluctuates for a coke powder content from 1.0% to 2.5%, reaching a maximum (88.61%) at 2.0%. However, variations in coke dosage had little effect on the TiO_2 content in the slag, and the residual reductant level was insufficient to significantly dilute the TiO_2 content. Maintaining a coke powder dosage of no greater than 2.0% in the treatment of pellet 2 ensures a high

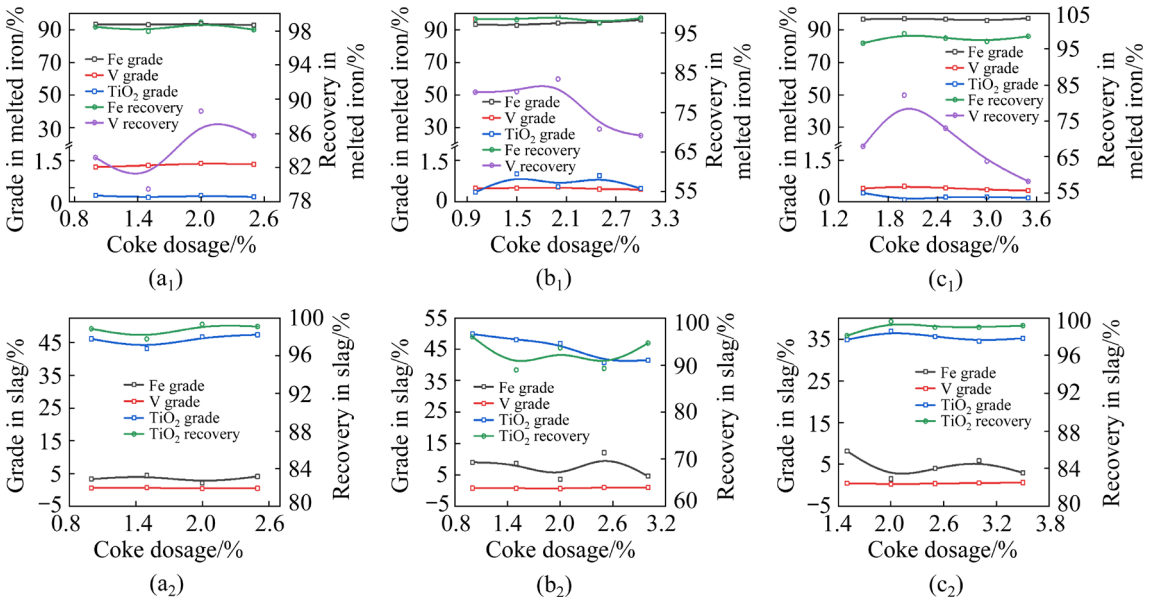

Fig. 9 Effect of coke dosage on reduction of VTM pellets in melted iron (a_1, b_1, c_1) and in slag (a_2, b_2, c_2): (a_1, a_2) Pellet 1; (b_1, b_2) Pellet 2; (c_1, c_2) Pellet 3

vanadium grade and level of recovery in melted iron. An increase in coke powder dosage to 3.0% was accompanied by a notable decrease in vanadium recovery from 83.48% to 69.22%. In the case of pellet 3, an increase in coke powder dosing resulted in an initial increase in vanadium recovery and subsequent decrease from a maximum of 82.17% to 58.15%. The melted iron grade in the iron water was relatively stable at approximately 96%. However, pellet 3 exhibited a high veinstone content and a low TiO_2 content. When the TiO_2 content in melted iron was as low as 0.06%, the TiO_2 grade in slag was 36.85%.

The results establish an optimum smelting separation coke dosage of 2.0% for pellets 1, 2, and 3.

4.2 Optimization of slag type

4.2.1 Effect of basicity

The effects of basicity on the smelting separation index for the three pellets were investigated under optimal operating conditions, generating the results shown in Fig. 10.

In the case of pellet 1, the iron grade in melted iron showed a clear increase (from 91.92% to 94.19%) with an increase in basicity (from 0.4 to 0.8). The TiO_2 grade also increased, from 0.43% to 1.3%. A constant level of TiO_2 (approximately 98%) in the slag was observed when the basicity was less than 0.4, but showed a decrease (approximately 93%) with increasing basicity. The recovery of vanadium in melted iron exhibited an increase from 76.12% at 0.4 basicity to 89.69% at 0.6 basicity with a vanadium grade of 0.37% in the latter case.

The vanadium grade increased from 0.48% to 0.53% in melted iron for pellet 2 when the basicity was increased from 0.11 to 0.4. This was accompanied by an increase in the recovery of vanadium from 76.81% to 83.48%. However, the vanadium recovery was lowered to 71.86% with a decrease in the grade to 0.46 in melted iron when the basicity was increased to 0.8. In addition, the TiO_2 grade in the slag exhibited a reduction of approximately 6% from its highest point, reaching 44.61%.

In the case of pellet 3, the iron grade first decreased and then increased with an increase in recovery rate from 97.98% to 99.94% with an increase in basicity from 0.08 to 0.6. At a basicity of 0.6, the iron grade in the slag is 0.7%, whereas the vanadium grade in the melted iron is 0.61%. This indicates that the majority of the vanadium oxides were reduced to melted iron during smelting separation, with a vanadium recovery of 88.52% in melted iron. The TiO_2 grade decreased from 36.46% to 35.90% in the slag with increasing basicity. However, a increase in basicity served to promote TiO_2 recovery in the slag, from 94.36% to 99.62%. At the same time, vanadium recovery in

the melted iron decreased to 77.95%, and the vanadium grade in the slag showed a twofold increase when the basicity was increased from 0.6 to 0.8. The TiO_2 grade in the slag fell below 35%.

Thermodynamic simulations and previous studies have indicated that excessive basicity increases the viscosity of the liquid phase and the reducibility of the slag-iron interface [34]. This enables a partial reduction of TiO_2 to melted iron, resulting in losses. The optimum smelting separation basicities for pellets 1, 2, and 3 are 0.4, 0.4, and 0.6, respectively.

Thermodynamic simulations and previous studies have indicated that excessive basicity increases the viscosity of the liquid phase and the reducibility of the slag-iron interface [34]. This enables a partial reduction of TiO_2 to melted iron, resulting in losses. The optimum smelting separation basicities for pellets 1, 2, and 3 are 0.4, 0.4, and 0.6, respectively.

4.2.2 Effect of MgO addition

The results of varying the MgO content on the smelting separation index for the three pellets are shown in Fig. 11.

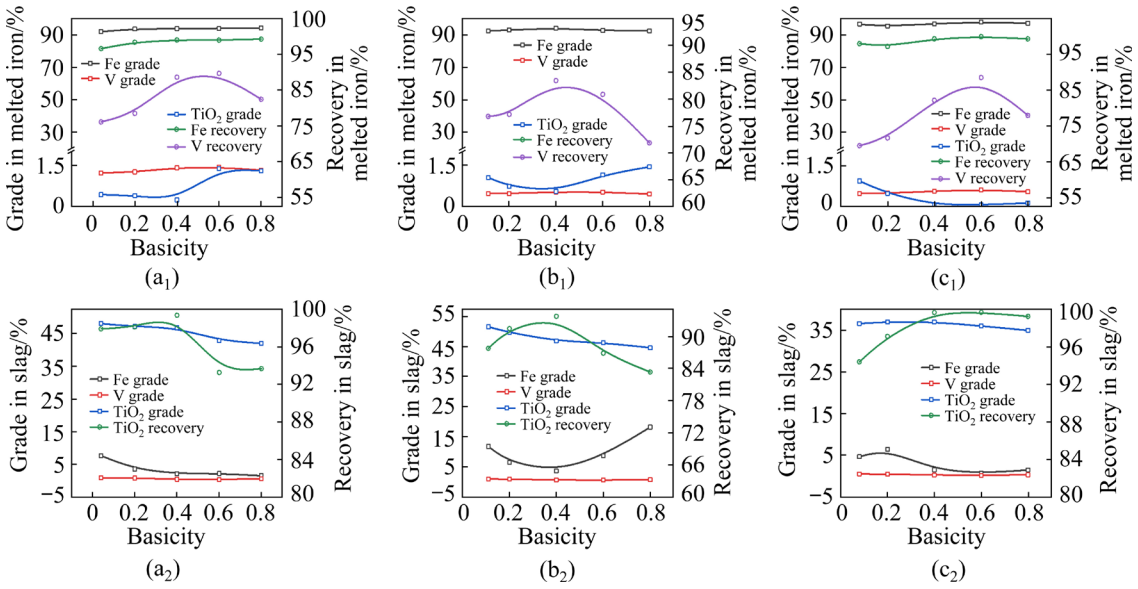

Fig. 10 Effect of basicity on reduction of VTM pellets in melted iron (a_1, b_1, c_1) and in slag (a_2, b_2, c_2): (a_1, a_2) Pellet 1; (b_1, b_2) Pellet 2; (c_1, c_2) Pellet 3

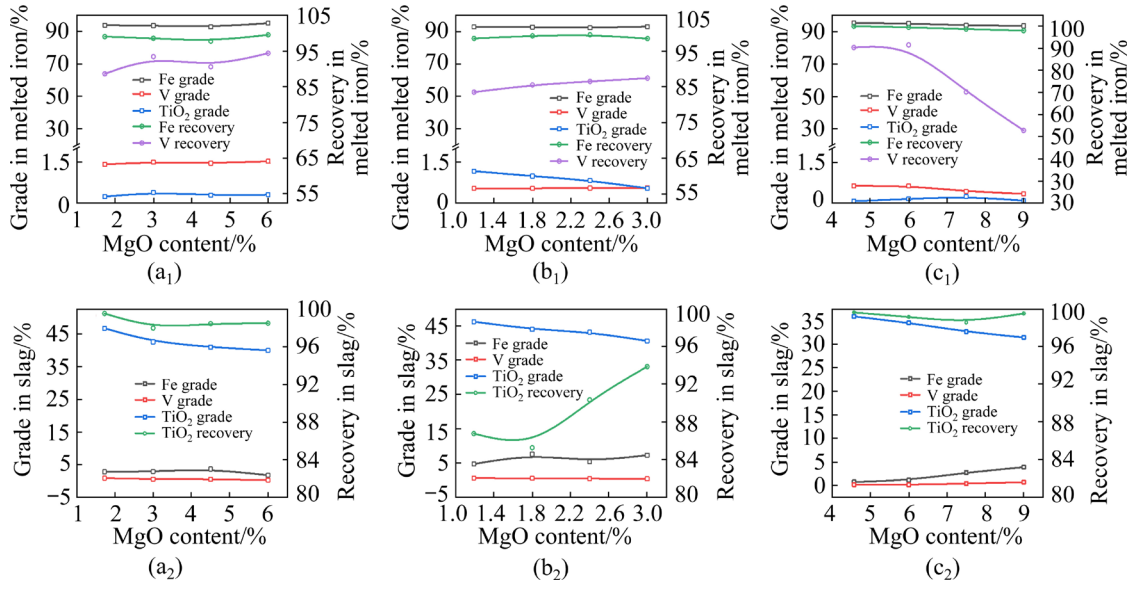

Fig. 11 Effect of MgO content on reduction of pre-reduced VTM pellets in melted iron (a_1, b_1, c_1) and in slag (a_2, b_2, c_2): (a_1, a_2) Pellet 1; (b_1, b_2) Pellet 2; (c_1, c_2) Pellet 3

In the case of pellet 1, the TiO_2 grade of the slag decreased from 46.77% to 42.61% with an increasing MgO content (from 1.73% to 3.0%). The melted iron vanadium grade reached 1.52% with a recovery of 94.38% at 6.0% MgO; the TiO_2 grade was less than 0.38%. The vanadium recovery in melted iron increased from 83.48% to 87.4% with increased MgO addition in pellet 2 from 1.19% to 3.0%. The TiO_2 grade in the slag exhibited a decrease of approximately 6%. However, the TiO_2 recovery showed a gradual increase, reaching 93.87% at 3.0% MgO. In the case of pellet 3, the TiO_2 decreased from 35.90% to 31.44% with increased MgO addition (from 4.57% to 9.0%). Moreover, the vanadium content in the slag increased from 0.17% to 0.68%. The experimental results have established that an increase in amount of MgO incorporated in the slag system promotes the recovery of vanadium and TiO_2. However, this results in a greater volume of slag and a reduction in the grade of TiO_2. An addition of 6%, 3% and 6% MgO in the case of pellets 1, 2, and 3, respectively, aligns with the simulation results.

The effect of the degree of metallization on the smelting separation indexes is presented in Fig. 12. Increasing the degree of metallization of pellet 1 from 75% to 89% resulted in a vanadium recovery increase from 81.77% to 94.38%; the vanadium grade in melted iron increased from 1.33% to 1.52%. At 85% metallization, the recovery of TiO_2 in the slag reached a maximum of 99.23%. In the case of pellet 2, the recovery of vanadium in melted iron increased from 79.54% to 92.63% with an increase in metallization from 75% to 92%. In addition, the vanadium grade in the slag decreased from 0.51% to 0.27%, and the TiO_2 grade increased from 31.62% to 40.59%. In the case of pellet 3, the TiO_2 grade in the melted iron was essentially unchanged, with a recovery of approximately 99% when the metallization level was increased from 74% to 90%. The vanadium recovery is higher than 91.46% at a metallization degree greater than 83%. However, the recovery of vanadium is only 85.5% at a metallization degree of 74%. In addition, the grade of vanadium in the melted iron exhibited a significant increase with an increase in the metallization degree.

The experimental results have demonstrated that an increase in metallization has a considerable impact on vanadium recovery. Conversely, it has a minimal effect on the recovery of TiO_2 in the slag, but contributes to an enhancement of grade. There is no significant influence on the grade of iron in melted iron. A high metallization degree facilitates the production of high-quality vanadium-bearing molten iron and titanium slag.

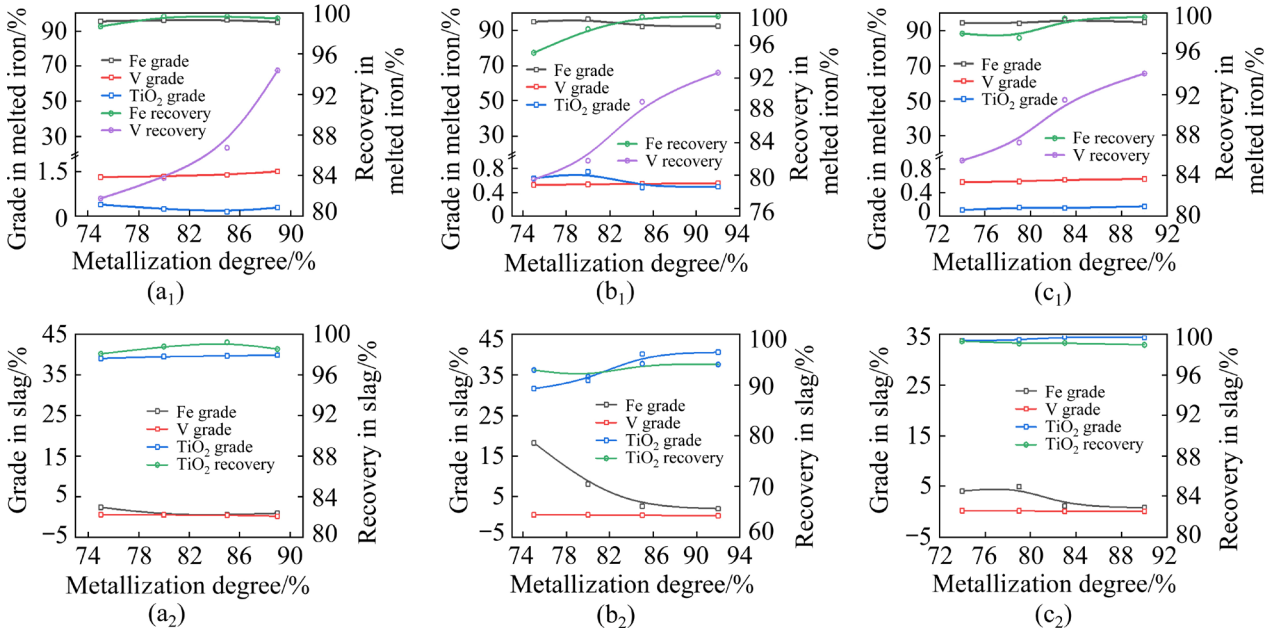

Fig. 12 Effect of metallization degree on reduction of pre-reduced VTM pellets in melted iron (a_1, b_1, c_1) and in slag (a_2, b_2, c_2): (a_1, a_2) Pellet 1; (b_1, b_2) Pellet 2; (c_1, c_2) Pellet 3

4.2.3 Effect of metallization degree on smelting separation

The results of smelting separation operated under the optimal regime are presented in Table 2. The degrees of metallization of pellets 1, 2, and 3 were 89%, 92%, and 90%, respectively. In the case of pellet 1, the highest vanadium grade is 1.52%, with a recovery of 94.38% and an iron recovery of 99.52%. A high iron grade of the raw material associated with pellet 2 resulted in the formation of an appreciable quantity of liquid iron during the smelting separation process. This liquid iron has the capacity to dissolve more carbon, reduce titanium oxides, and dissolve TiO_2 in melted iron, resulting in a loss of TiO_2. Consequently, the TiO_2 grade in melted iron reaches 0.50%, and the TiO_2 recovery rate is 94.08%. Pellet 3 exhibited an iron recovery of up to 99.60%, with a TiO_2 recovery up to 98.96%.

4.3 Product analysis

4.3.1 Vanadium-bearing molten iron

The results of the chemical elemental analysis are shown in Table 3. The melted iron associated with pellet 1 has a vanadium grade of 1.52%, an iron grade of 95.06%, a carbon content of 2.49%, and a low impurity content. Pellet 2 exhibits a 92.35% iron grade, with a carbon content of 5.19% and vanadium and TiO_2 grades of 0.56% and 0.50%, respectively. Pellet 3 has an iron grade of 94.79%, a vanadium grade of 0.63%, a TiO_2 content of 0.17%, and a carbon content of 4.07%, with a low impurity content. The three forms of vanadium-bearing molten iron exhibit iron grades above 92%, titanium contents below 0.3%, vanadium contents reaching a maximum of 1.56%, and carbon contents of approximately 5% in the iron component.

The high temperature of the graphite crucible results in carbon infiltration into the melted iron, leading to a low melted iron grade. In industrial production, contamination of slag and melted iron by impurities in the refractory can be effectively avoided in operations such as slag hanging. Therefore, it is reasonably anticipated that quality of industrially produced melted iron will be higher than that of the vanadium-bearing iron obtained in this laboratory study.

Figure 13 shows the XRD patterns of melted iron obtained from the melting separation experiments of the three VTM pellets. The iron phase composition shows slight differences, but the principal phase is metallic iron. In addition, a quartz phase and trace perovskite are present in pellet 1 and pellet 2. The SEM-EDS analysis (Fig. 14) provides evidence of TiC formation and carbon diffusion into the melted iron at the fissures in pellet 1. Analysis of point 1 reveals a 95.51% iron, 0.11% Ti and 0.40% V content. The analysis of point 2 indicates a substantial presence of vanadium and titanium, with 1.85% Fe, 29.33% V, 55.34% Ti, and 13.41% C. The location of vanadium in pellet 2 is essentially identical to that of Fe. The dissolved TiC in Fe is higher than that in pellet 3, which is consistent with the chemical composition data. In addition, TiC and SiC are predominantly concentrated in the carburization area, with a minimal presence

Table 2 Comparison of results for three pellets under optimal smelting separation processing

Pellet	Grade/%						Recovery/%		
	In melted iron			In slag					
	Fe	V	TiO_2	Fe	V	TiO_2	Fe	V	TiO_2
1	95.06	1.52	0.30	0.89	0.18	39.89	99.52	94.38	98.55
2	92.35	0.56	0.50	2.01	0.27	40.59	99.58	92.63	94.08
3	94.79	0.63	0.17	0.83	0.08	34.37	99.60	94.06	98.96

Table 3 Chemical composition of melted iron under optimal smelting separation processing (wt.%)

Pellet	Fe	C	TiO_2	V	CaO	SiO_2	MgO	Al_2O_3	P	S
1	95.06	2.49	0.30	1.52	0.026	0.20	0.014	0.011	0.015	0.016
2	92.35	5.19	0.50	0.56	0.0034	0.44	0.035	0.04	0.029	0.023
3	94.79	4.07	0.17	0.63	0.0036	0.16	0.013	0.0076	0.0078	0.017

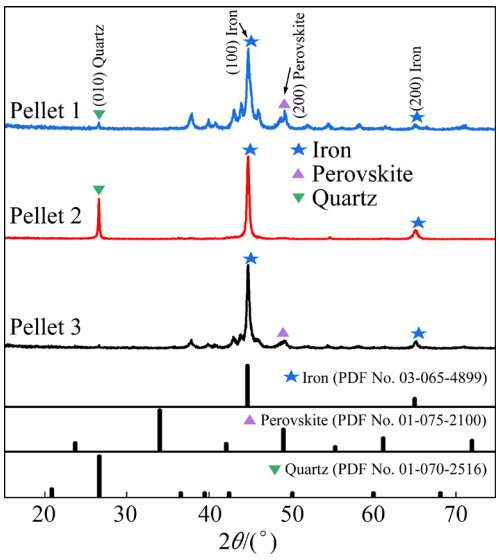

Fig. 13 XRD patterns of melted iron from three pre-reduction pellets smelting separation systems

of other impurities. The majority of vanadium in pellet 3 is dissolved in the metallic iron phase, and the vanadium-bearing molten iron has a very low sulfur content. This suggests that the vanadium and titanium resulting from the smelting separation process are more effectively managed, enabling the incorporation of vanadium into the melted iron and preventing the reduction of titanium.

4.3.2 Smelting separation of titanium slag

The chemical composition of the titanium slag is presented in Table 4, with the exception of pellet 3, where the TiO_2 content is 34.37%. In contrast, pellets 1 and 2 exhibited a TiO_2 content exceeding 39%. The iron content of pellet 1 and pellet 3 is less than 1%, and is higher (2.01%) in pellet 2.

The XRD analysis results, as shown in Fig. 15, indicate that the primary phases in the molten titanium slag are anosovite and a spinel, with

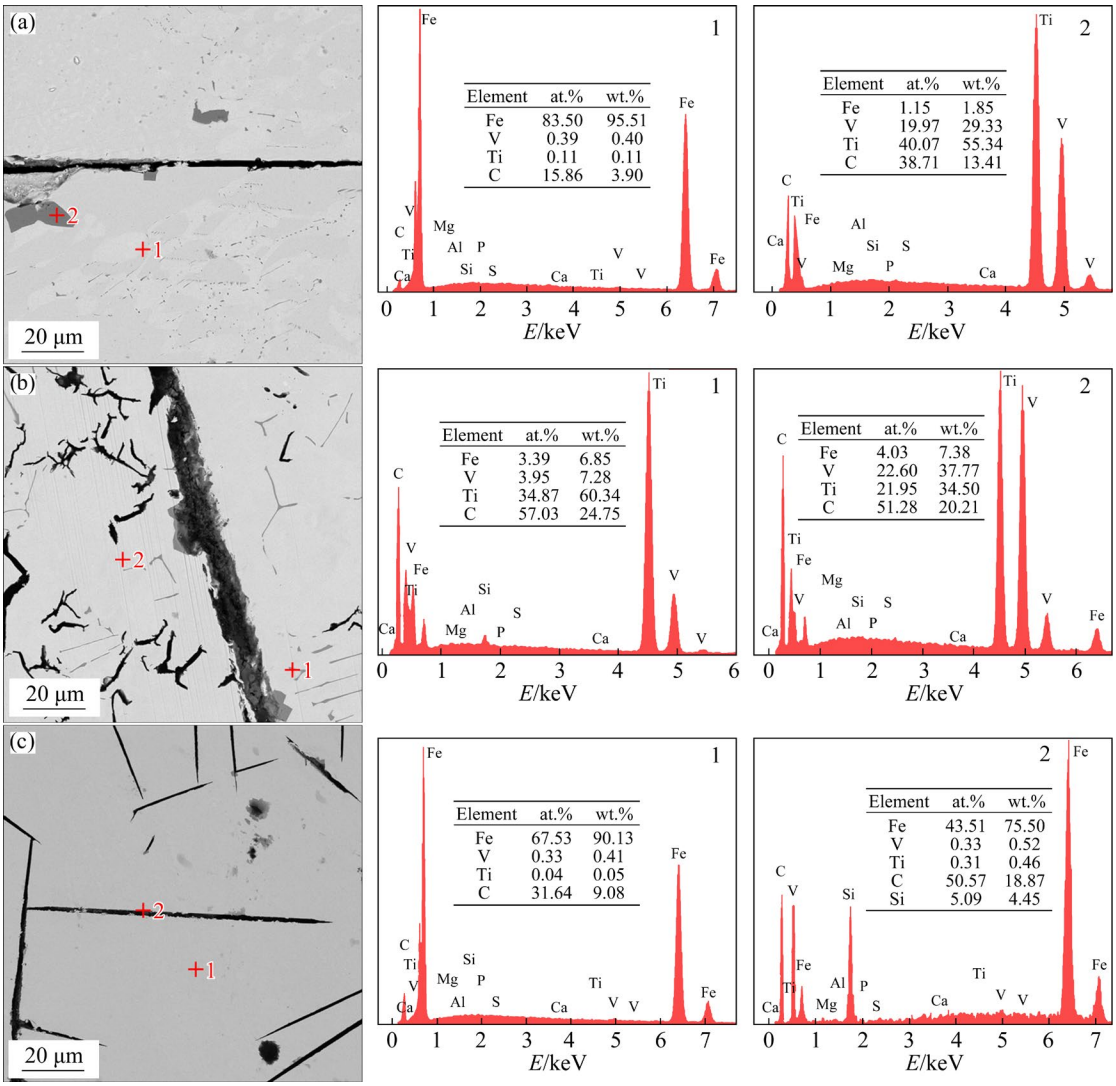

Fig.14 SEM−EDS analyses of melted iron from three pre-reduction pellets smelting separation systems: (a) Pellet 1; (b) Pellet 2; (c) Pellet 3

Table 4 Chemical composition of titanium slag under optimal smelting separation processing (wt.%)

Pellet	Fe	TiO_2	V	CaO	SiO_2	MgO	Al_2O_3	P	S
1	0.89	39.89	0.18	6.98	17.39	17.85	15.58	0.023	0.040
2	2.01	40.59	0.27	4.92	12.36	17.55	18.36	0.0089	0.073
3	0.83	34.37	0.08	11.05	18.42	18.38	14.02	0.0041	0.062

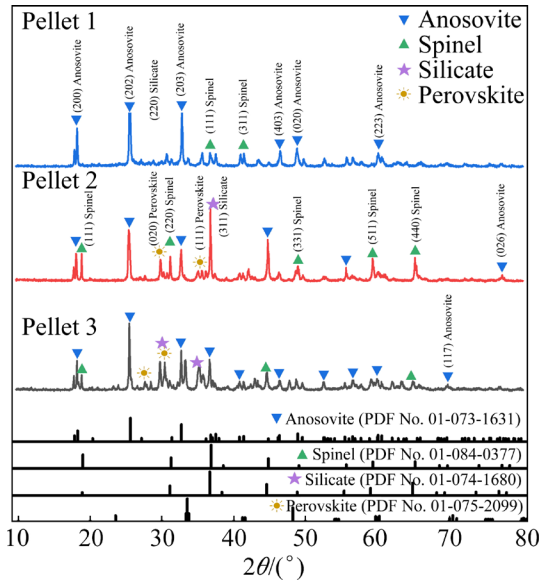

Fig. 15 XRD patterns of titanium slag from three pre-reduction pellets smelting separation

silicate and perovskite. As shown in Fig. 16, the main impurities in the titanium slag from the three pellets are silica, alumina, calcium oxide, and magnesium oxide. In the case of pellet 1, the orientation of vanadium and titanium in the slag is similar. The majority of vanadium that does not enter the melted iron is present in the black titanite phase. A minor amount of titanium is also present in the spinel and silicate phases. The orientation of calcium, magnesium, and silicon is also similar. Titanium in pellet 2 is present mainly as a black titanium ore, with minor amounts in the perovskite and silicate phases, where the trends for vanadium and titanium are similar. In the case of pellet 3, titanium is predominantly present in the black titanite phase, with minor amounts in the perovskite, spinel, and silicates. Silicates have an approximate titanium content similar to that of the spinel, and are virtually free of vanadium.

5 Conclusions

(1) Phase analysis reveals that valuable elements in pellets 1, 2, and 3 are predominantly present as metallic iron and ilmenite, where vanadium is associated with iron and silicates, and gangue as silicates and peridotite (Ca and Mg) surrounding iron grains.

(2) Thermodynamic simulations using FactSage indicate that $FeTi_2O_5$ converts to TiC at low temperatures, which must be suppressed. The melting temperature and viscosity decrease with increasing basicity. The addition of MgO increases the melting temperature but lowers viscosity. Optimal slag conditions (basicity 0.4−0.6 and 17.5%−19% MgO) favor high-TiO_2 phases such as $MgTi_2O_5$ and $CaTiO_3$.

(3) The optimum melting separation temperatures for pellets 1, 2, and 3 are 1690, 1610, and 1590 °C, with 20−25 min smelting and 2% coke addition. These conditions serve to enhance liquid phase fluidity, vanadium migration to melted iron (>90% recovery), and TiO_2 retention in the slag at basicity 0.4−0.6 and MgO 3.0%−6.0%, and the pellet metallization exceeds 88%. The smelting process for vanadium−titanium magnetite (VTM) reduces slag basicity while achieving >90% vanadium recovery, retaining titanium in ilmenite-rich slag, which is suitable for high-quality TiO_2 production via sulfuric acid processing after leaching.

CRediT authorship contribution statement

Zheng-qi GUO: Data curation, Conceptualization, Writing – Review & editing; **Xing CHEN:** Methodology, Investigation, Writing – Original draft; **Yue SHI:** Conceptualization, Investigation, Writing – Review & editing; **De-qing ZHU:** Validation, Project administration; **Jian PAN:** Validation, Project administration; **Cong-cong YANG:** Resources, Methodology, **Si-wei LI:** Formal analysis; **Ji-wei XU:** Resources; **Xin WANG:** Investigation.

Declaration of competing interest

The authors declare that they have no known competing financial interests or personal relationships that could have appeared to influence the work reported in this paper.

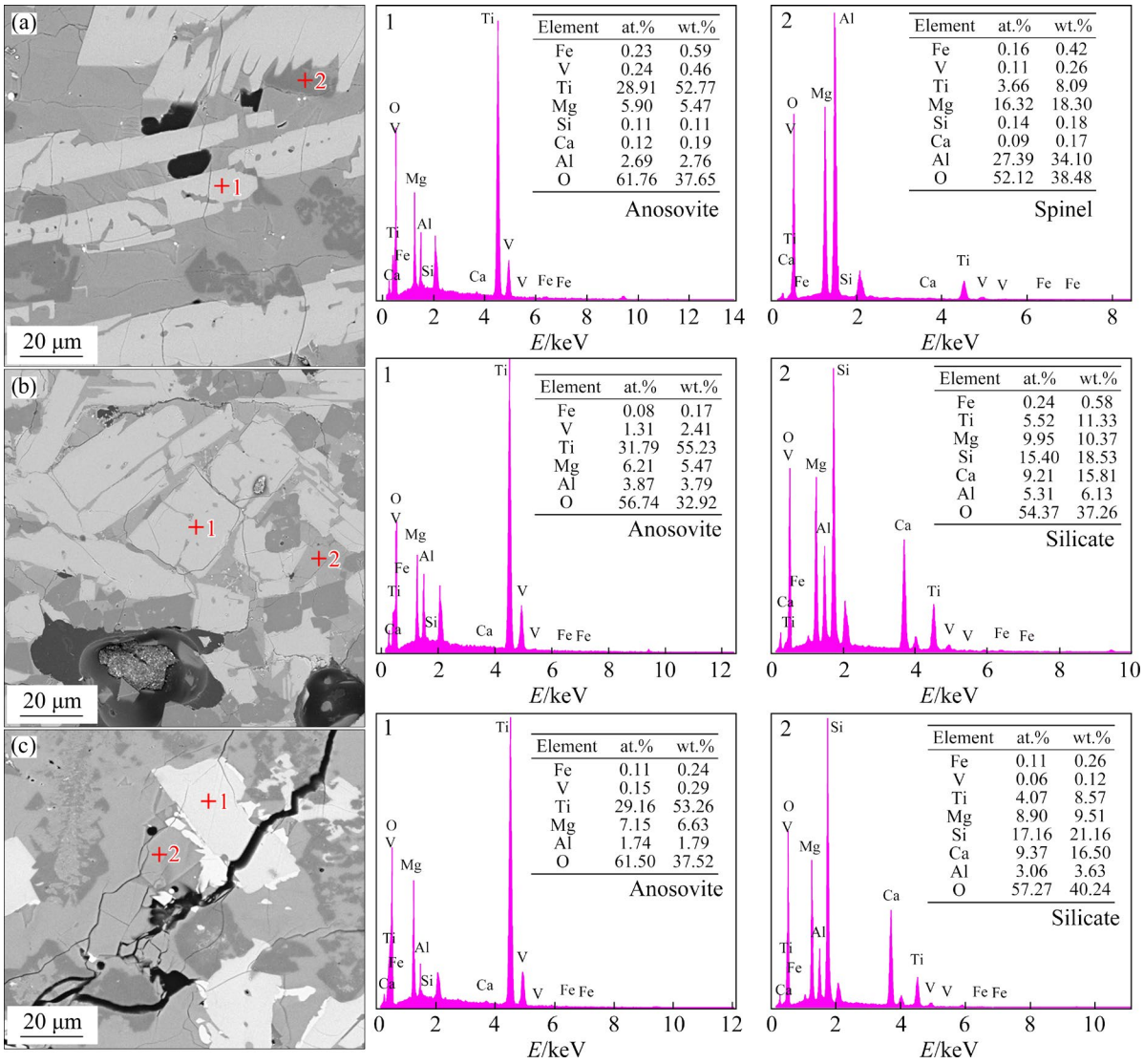

Fig. 16 SEM−EDS analyses of titanium slag from three pre-reduction pellet smelting separation: (a) Pellet 1; (b) Pellet 2; (c) Pellet 3

Acknowledgments

The authors sincerely appreciate the financial support from the National Key R&D Program of China (Nos. 2023YFC3903900, 2023YFC3903904), and the National Natural Science Foundation of China (Nos. 52274343, 52174329). They also extend gratitude to Scientific Compass (www.shiyanjia.com) for providing invaluable assistance with the XRD analysis.

References

[1] SHI Yue, ZHU De-qing, PAN Jian, GUO Zheng-qi, LU Sheng-hu, XUE Yu-xiao. Investigation into the coal-based direct reduction behaviors of various vanadium titanomagnetite pellets [J]. Journal of Materials Research and Technology, 2022, 19: 243−262.

[2] HU Cheng, YANG Zhen-dong, HE Miao, ZHAN Ya-zhi, ZHANG Zhen-yu, PENG Cong, ZENG Li, LIU Yong-hong, YANG Zhao-yue, YIN Hua-qun, LIU Zheng-hua. From waste to wealth: Current advances in recycling technologies for metal recovery from vanadium-titanium magnetite tailings [J]. Journal of Sustainable Metallurgy, 2024, 10(3): 1007−1035.

[3] ZHAO Long-sheng, WANG Li-na, CHEN De-sheng, ZHAO Hong-xin, LIU Ya-hui, QI Tao. Behaviors of vanadium and chromium in coal-based direct reduction of high-chromium vanadium-bearing titanomagnetite concentrates followed by magnetic separation [J]. Transactions of Nonferrous Metals Society of China, 2015, 25(4): 1325−1333.

[4] HAN Ji-qing, ZHANG Jing, ZHANG Jia-hao, CHEN Xiao, ZHANG Li, TU Gan-feng. Recovery of Fe, V, and Ti in modified Ti-bearing blast furnace slag [J]. Transactions of Nonferrous Metals Society of China, 2022, 32(1): 333−344.

[5] XIANG Jun-yi, HUANG Qing-yun, LV Xue-wei, BAI Chen-guang. Multistage utilization process for the gradient-recovery of V, Fe, and Ti from vanadium-bearing

converter slag [J]. Journal of Hazardous Materials, 2017, 336: 1−7.

[6] SUN Hao-yan, WANG Jing-song, DONG Xiang-juan, XUE Qing-guo. A literature review of titanium slag metallurgical processes [J]. Metalurgia International, 2012, 17(7): 49−56.

[7] FAN Gang-qiang, WANG Meng, DANG Jie, ZHANG Run, LV Ze-peng, HE Wen-chao, LV Xue-wei. A novel recycling approach for efficient extraction of titanium from high-titanium-bearing blast furnace slag [J]. Waste Management, 2021, 120: 626−634.

[8] LIU Shi-yuan, WANG Li-jun, CHEN Jun, YE Lin, DU Jun-yan. Research progress of vanadium extraction processes from vanadium slag: A review [J]. Separation and Purification Technology, 2024, 342: 127035.

[9] ZHANG Xue-fei, FANG De-an, SONG Shi-zhe, CHENG Gong-jin, XUE Xiang-xin. Selective leaching of vanadium over iron from vanadium slag [J]. Journal of Hazardous Materials, 2019, 368: 300−307.

[10] GILLIGAN R, NIKOLOSKI A N. The extraction of vanadium from titanomagnetites and other sources [J]. Minerals Engineering. 2020, 146: 106106.

[11] SAMANTA S, MUKHERJEE S, DEY R. Oxidation behaviour and phase characterization of titaniferous magnetite ore of eastern India [J]. Transactions of Nonferrous Metals Society of China, 2014, 24(9): 2976−2985.

[12] JENA M S, TRIPATHY H K, MOHANTY J K, MOHANTY J N, REDDY P S R. Roasting followed by magnetic separation: A process for beneficiation of titano-magnetite ore [J]. Separation Science and Technology, 2015, 50(8): 1221−1229.

[13] WANG Ming-yu, ZHOU Sheng-fan, WANG Xue-wen, CHEN Bian-fang, YANG Hao-xiang, WANG Sai-kuai, LUO Peng-fei. Recovery of iron from chromium vanadium-bearing titanomagnetite concentrate by direct reduction [J]. JOM, 2016, 68(10): 2698−2703.

[14] SUI Yu-lei, GUO Yu-feng, JIANG Tao, QIU Guan-zhou. Separation and recovery of iron and titanium from oxidized vanadium titano-magnetite by gas-based reduction roasting and magnetic separation [J]. Journal of Materials Research and Technology, 2019, 8(3): 3036−3043.

[15] WANG Shuai, GUO Yu-feng, JIANG Tao, CHEN Feng, YANG Ling-zhi, JIANG Tao, QIU Guan-zhou. Behavior of titanium during the smelting of vanadium titanomagnetite metallized pellets in an electric furnace [J]. JOM, 2019, 71(1): 323−328.

[16] WANG Shuai, GUO Yu-feng, JIANG Tao. Reduction behaviors of iron, vanadium and titanium oxides in smelting of vanadium titanomagnetite metallized pellets [J]. JOM, 2017, 69(9): 1646−1653.

[17] SHI Quan, TANG Jue, CHU Man-sheng. High-efficiency smelting separation of vanadium–titanium magnetite by electrothermal smelting: Parameter optimization and element enrichment mechanism [J]. Journal of Sustainable Metallurgy, 2023, 9(3): 1126−1138.

[18] SUN Yu, ZHENG Hai-yan, DONG Yue, JIANG Xin, SHEN Yan-song, SHEN Feng-man. Melting and separation behavior of slag and metal phases in metallized pellets obtained from the direct-reduction process of vanadium-bearing titanomagnetite [J]. International Journal of Mineral Processing, 2015, 142: 119−124.

[19] WANG Shuai, LI Guang, GUO Yu-feng, CHEN Feng, JING Jian-fa, ZHANG Jin-lai, YANG Ling-zhi, QIU Guan-zhou. Effects of MnO on the smelting process of vanadium titanomagnetite pre-reduced pellets in an electric furnace [J]. Journal of Materials Research and Technology, 2022, 20: 2262−2270.

[20] LIU Zhao-yang, WANG Bo, DING Xue-yong. Optimizing pre-reduction of vanadium–titanium magnetite through recycling and integrating of top gas from melting furnace and tail gas from rotary kiln [J]. Process Safety and Environmental Protection, 2024, 185: 86−95.

[21] TONG Shuai, AI Li-qun, HONG Lu-kuo, SUN Cai-jiao, LI Ya-qiang, YUAN Yi-pang. Reduction of Chengde vanadium titanium magnetite concentrate by microwave enhanced Ar−H2 atmosphere [J]. International Journal of Hydrogen Energy, 2024, 49: 42−48.

[22] YI Yi-hui, SUN Hu, YOU Jin-xiang, ZHANG Jin, CAI Yuan, ZHANG Xin, LUO Jun, QIU Guan-zhou. Vanadium recovery from Na_2SO_4-added V−Ti magnetite concentrate via grate-kiln process [J]. Transactions of Nonferrous Metals Society of China, 2022, 32(6): 2019−2032.

[23] NIE Wen-lin, WEN Shu-ming, LIU Dian-wen, HU Tu, ZHANG Libo. Innovative application of two-stage sulfuric acid leaching for efficient recovery of Ti from titanium-bearing electric furnace slag [J]. Journal of Environmental Chemical Engineering, 2023, 11(1): 109174.

[24] JIAO Ke-xin, ZHANG Jian-liang, WANG Zhi-yu, CHEN Chun-lin, LIU Yan-xiang. Effect of TiO_2 and FeO on the viscosity and structure of blast furnace primary slags [J]. Steel Research International, 2017, 88(5): 1600296.

[25] ZHOU Hang-hang, GUO Jia, HOU Yong, DANG Jie, ZHANG Shuo, LV Xue-wei. Molecular dynamics simulation, spectroscopy characterization and properties testing of high-titanium $CaO-SiO_2-10wt.\%MgO-13wt.\%Al_2O_3-4wt.\%FeO-40wt.\%TiO_2$ slag melts [J]. Journal of Alloys and Compounds, 2024, 1002: 175444.

[26] BALE C W, BÉLISLE E, CHARTRAND P, et al. Reprint of: FactSage thermochemical software and databases, 2010−2016 [J]. Calphad, 2016, 55: 1−19.

[27] WANG Shuai, GUO Yu-feng, JIANG Tao, CHEN Feng, ZHENG Fu-qiang, TANG Min-jun, YANG Ling-zhi, QIU Guan-zhou. Appropriate titanium slag composition during smelting of vanadium titanomagnetite metallized pellets [J]. Transactions of Nonferrous Metals Society of China, 2018, 28(12): 2528−2537.

[28] YE Miao-ting, BU Nai-jing, CHEN Lai, LI Rong, ZHEN Qiang. Study on reaction mechanism for the synthesis of vanadium nitride by carbothermic reduction nitridation method [J]. Ceramics International, 2024, 50(5): 7458−7468.

[29] LIU Shui-shi, GUO Yu-feng, QIU Guan-zhou, JIANG Tao, CHEN Feng. Solid-state reduction kinetics and mechanism of pre-oxidized vanadium–titanium magnetite concentrate [J]. Transactions of Nonferrous Metals Society of China, 2014, 24(10): 3372−3377.

[30] ZENG Rui-qi, LI Wei, WANG Nan, FU Gui-qin, CHU Man-sheng, ZHU Miao-yong. Effect of Al_2O_3 on the gas-based direct reduction behavior of Hongge vanadium

titanomagnetite pellet under simulated shaft furnace atmosphere [J]. Powder Technology, 2020, 376: 342−350.

[31] TANG Jue, CHU Man-sheng, LI Feng, TANG Ya-ting, LIU Zheng-gen, XUE Xiang-xin. Reduction mechanism of high-chromium vanadium−titanium magnetite pellets by H_2−CO−CO_2 gas mixtures [J]. International Journal of Minerals, Metallurgy, and Materials, 2015, 22(6): 562−572.

[32] TANG Jue, CHU Man-sheng, FENG Cong, LI Feng, LIU Zheng-gen. Phases transition and consolidation mechanism of high chromium vanadium-titanium magnetite pellet by oxidation process [J]. High Temperature Materials and Processes, 2016, 35(7): 729−738.

[33] TANG Jun, CHU Man-sheng, FENG Cong, TANG Ya-ting, LIU Zheng-gen. Melting separation behavior and mechanism of high-chromium vanadium-bearing titanomagnetite metallized pellet got from gas-based direct reduction [J]. ISIJ International, 2016, 56(2): 210−219.

[34] KIM H, MATSUURA H, TSUKIHASHI F, WANG W L, MIN D J, SOHN I. Effect of Al_2O_3 and CaO/SiO_2 on the viscosity of calcium-silicate-based slags containing 10 mass Pct MgO [J]. Metallurgical and Materials Transactions B Process Metallurgy and Materials Processing Science, 2013, 44(1): 5−12.

不同钒钛磁铁矿还原球团的熔分行为

郭正启[1]，陈 兴[1]，石 玥[2]，朱德庆[1]，潘 建[1]，杨聪聪[1]，李思唯[1]，徐继伟[1]，王 欣[1]

1. 中南大学 资源加工与生物工程学院，长沙 410083；
2. 河南科技大学 材料科学与工程学院，洛阳 471000

摘 要：为了从钒钛磁铁矿中高效提取钒和钛，系统探讨钒钛磁铁矿球团的熔分行为。通过 Factsage 模拟与实验分析来自不同区域的 3 种预还原球团的熔炼分离行为。模拟结果表明，$FeTi_2O_5$ 在低温下会转化为 TiC，需加以抑制。在最佳条件(温度 1590~1690 ℃、时间 20~25 min、焦粉添加量 2%、碱度 0.4~0.6、MgO 含量 3.0%~6.0%)下的实验结果显示，铁的品位为 92.35%~95.06%，钛的品位为 34.37%~39.89%，钒的品位为 0.56%~1.52%，其回收率分别为 99.52%~99.60%、94.08%~98.96%和 92.63%~94.38%。矿渣中钛主要以钙钛矿形式存在，适用于硫酸法钛白粉生产。提高碱度、MgO 含量及球团金属化率可提高铁水中钒的回收率，但会降低矿渣中钛的品位。在优化条件下，该工艺可有效利用钒钛资源。

关键词：钒钛磁铁矿；球团预还原；熔分；钛渣利用

(Edited by Xiang-qun LI)